Gravity high detected southeast of the vicinity coincides with the distribution of Dalupirip metamorphic rocks with density of 2.78.

And lastly, high gravity zone in the eastern edge of the area reflects the Pugo formation with density of 2.78.

3–5–2 Residual Gravity

Filtered map of λ=0.25 with a wave length of 1 km was used to determine the geological noise and scattering of the data.

Figure II–3–12, residual map of λ=0.25 – 0.1 and wave length of 1 ~ 2.9 km expresses the sub-surface structure shallower than 1,500 m.

This map implies more clearly the geological structure than the Bouguer anomaly map. The not so eminent gravity highs around Acupan mine indicate the intrusive rocks of Virac granodiorite (p=2.82), Antamok diorite and gabbro (p=2.76).

Furthermore, a fault-like pattern running 5 km in N–S trend was inferred to exist between gravity highs and lows in the southeastern part of the area.

Fig. II–3–13, Residual map of λ=2.1 – 10.2 with corresponding wave length of 2.9 – 6.4 km reflects the structure down to 3 km depth.

The map showed center of gravity lows north of Itogon which tend to spread in N–S direction. This anomaly pattern resembles the distribution of Itogon quartz diorite at depth.

Meanwhile, high anomalies in the southwest and eastern edge of the area are extension of the Zigzag and Pugo formations, respectively.

Northwestern high anomaly, on the other hand, connotes the extension at depth of the same intrusive rock described in Fig. II–3–12.

Fig. II–3–14, Residual map of λ=10.2 with a wavelength of 6.4 km is a kind of high-cut-filter map indicating the deeper structures (> 3 km). It showed high gravity values in the west that decrease towards southeast. The low gravity values were located within the uplifted zone which are not typical of low gravity anomalies, hence it is somewhat vague as to what this anomaly suggests.

Furthermore, no prominent structures related with geothermal system were detected in each filtered map.

3–5–3 Vertical Secondary Derivative

The area is characterized by a series of volcanic activity evidenced by the presence of several plugs and uplifted zones. To delineate the different rock types, a vertical second derivative was utilized in the data processing.

Fig. II–3–15 is a vertical second derivative map wherein the solid contour lines (Gv=0) appear to coincide well with the geological setting. Intrusive rocks sorrounding Balatoc plug are separated into two by ENE – WSW and WNW – ESE lines.

CHAPTER 4 ELECTRICAL SURVEY

CHAPTER 4 ELECTRICAL SURVEY

4–1 Purpose of the Survey

The electrical resistivity survey is most commonly used in the Philippines as a geophysical exploration technique particularly in the early stages of geothermal surveys.

Basically, rock is electrically a poor conductor. It becomes a good conductor when its pores and fissures are filled with good conductive fluids. It is through this type of surveys where these conductive zones or the geothermal heated zones are usually delineated even in the absence of extensive surface manifestations.

Since the conductivity or resistivity of rock layers depend on the water in its pores and fissures, the amount of water that it contained and the ionic mobility in the water; it is therefore proportional to the pore water and to the varying temperature. Thus, resistivity decreases as the temperature increases as shown in the following relationship:

$$\rho_f = \frac{m\rho_{f\,18}}{1 + 0.025\,(t - 18)} \quad (\Omega m)$$

where ρ_f = resistivity of beds (Ω-m)

ρ_{f18} = resistivity at temperature of 18°C

m = commutation factor

t = temperature

Resistivity of rock layers (beds) are not only dependent on their porosity and temperature but also on their NaCl concentration and clay mineral contents. The relationship between NaCl concentration and resistivity using the Schlumberger method is shown in Fig II–4–1.

Generally, compact crystalline rocks and silicified zones have high resistivity while argillized rocks such as claybeds with high porosity have low resistivity. Since resistivities of rocks in different areas show different values, physical property measurements and resistivity logging of rocks in the area were made to determine this differences. The results of measurements on the samples collected in the area are discussed in 4–3–1.

Benguet Corporation, Itogon-Suyoc Mines and other gold mining firms operate in the Acupan-Itogon area. Since the electrical noises produced by underground operations in these mines are very strong, resistivity sounding by Schlumberger configuration is not advisable. Thus, an especially designed signal enhanced receiver was adopted for the survey.

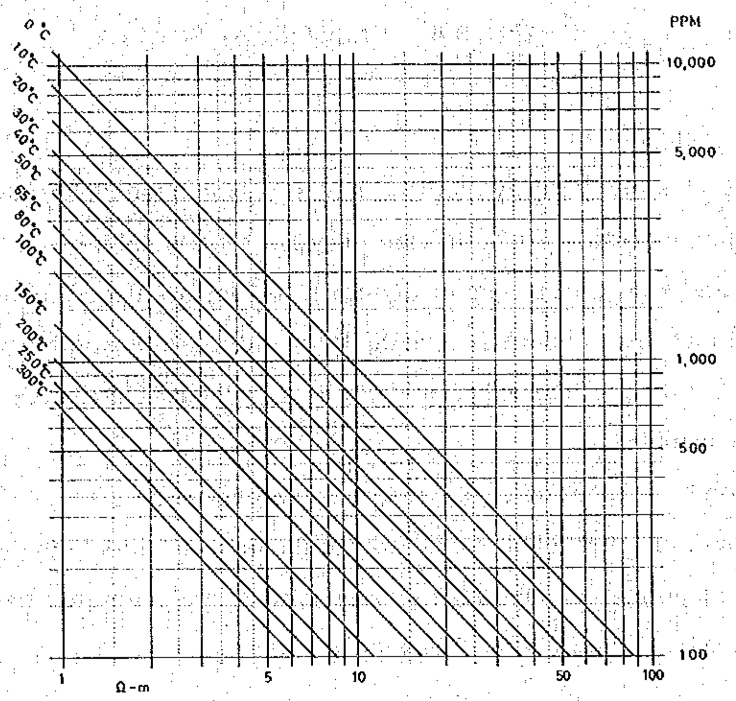

Fig. II–4–1 Resistivity Graph for Salinity and Temperature of NaCl Solution

4–2 Method of Survey

Due to steep topography and rugged terrain, the reconnaissance resistivity survey was conducted along the roads to cover most part of the area.

The resistivity arrays used were Schlumberger, dipole-dipole, pole-dipole, and bipole-dipole methods depending upon the position of the current and potential electrodes as they are set on the ground during the course of the survey.

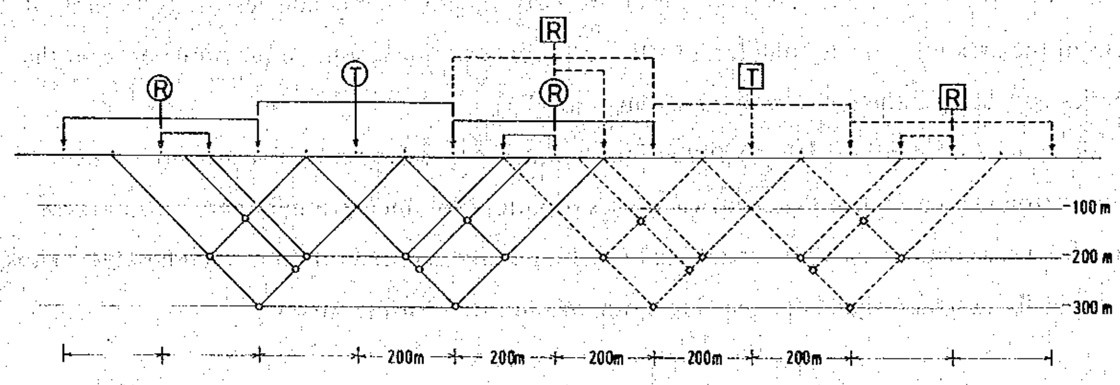

Fig. II–4–2 Electrode Configuration and Pseudo Section

Most of the measurements were carried out using the dipole-dipole array with interval (a) of 100 meter; separation factor (n) of 1 and 2 and depth of penetration of 200–400 meters below ground surface. Deeper informations can be obtained by increasing the spacing between current and potential electrodes. However, when the spacing exceeds 200 meters the input signal in the receiver becomes smaller thereby increasing the effect of noise. With decreased signal-to-noise ratio (S/N) it becomes difficult to carry out the resistivity measurements. Hence, only the two electrode spacings (n) were adopted to measure the resistivity as broad and deep as possible.

The resistivity ρ is calculated by the following equation when coordinates of current and potential electrodes are C_1 (x_1, y_1), C_2 (x_2, y_2) and P_1 (x_3, y_3), P_2 (x_4, y_4) respectively.

$$\rho = K \cdot \frac{V}{I} \quad (\Omega\text{-m})$$

$$k = 2\pi / \left(\frac{1}{C_1P_1} - \frac{1}{C_1P_2} - \frac{1}{C_2P_1} + \frac{1}{C_2P_2} \right)$$

where K = electrode configuration factor

V = potential in volt

I = current in ampere

The apparent resistivities (ρ) were calculated by feeding into the computer the x–y co-ordinates of each measuring points, the measured potential V, and current I applied to the ground.

4–2–1 Noise Measurement

Noise monitoring was first conducted before the actual resistivity survey to determine the electrical disturbance generated from the mining site in the survey area that can affect the sensitivity of the receiver and hence, the actual resistivity values.

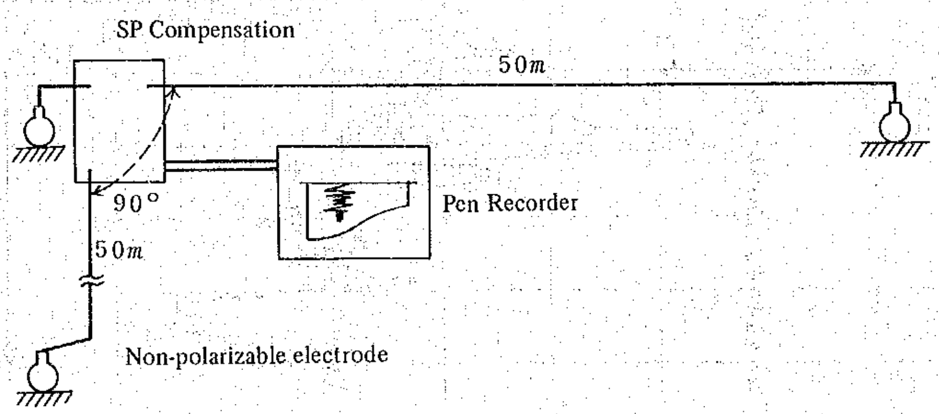

This was done by placing two lines placed 90° with each other with the electrodes spaced 50 meters and oriented such that it faces the direction of the suspected noise source.

The self-potential measured were compensated by SP bucking circuit such that only the noise change is measured. The measuring system and electrode array are shown below.

Based on this monitoring survey, electrical as well as cultural noises exceeded 200 mv especially near the mining sites due to the on-and-off operation of the tramcars underground. Noise levels were also measured on Sunday evenings when mining operations temporarily stop but still up to 10 mv of noise were recorded. The noise wave forms are shown in Fig II–4–3.

This recorded noise is very strong compared with the expected receiver signal of about 2 mv in anomalous areas. From the graphs, most of the noises seem to be in the DC ranges.

From this, ordinary direct-current method of electrical survey usually adopted for geothermal areas is not applicable in this particular area.

In order to minimize these noises, a 3Hz transmitter signal was used. The received signal at the potential electrodes is then passed through a sharp band-pass filter before connecting it to the input of the receiver unit. This filter eliminates noises below and above the 3Hz signal which include the AC and excessive DC noises. Thus, only the weak transmitter signal with its varying amplitude is detected at the receiver.

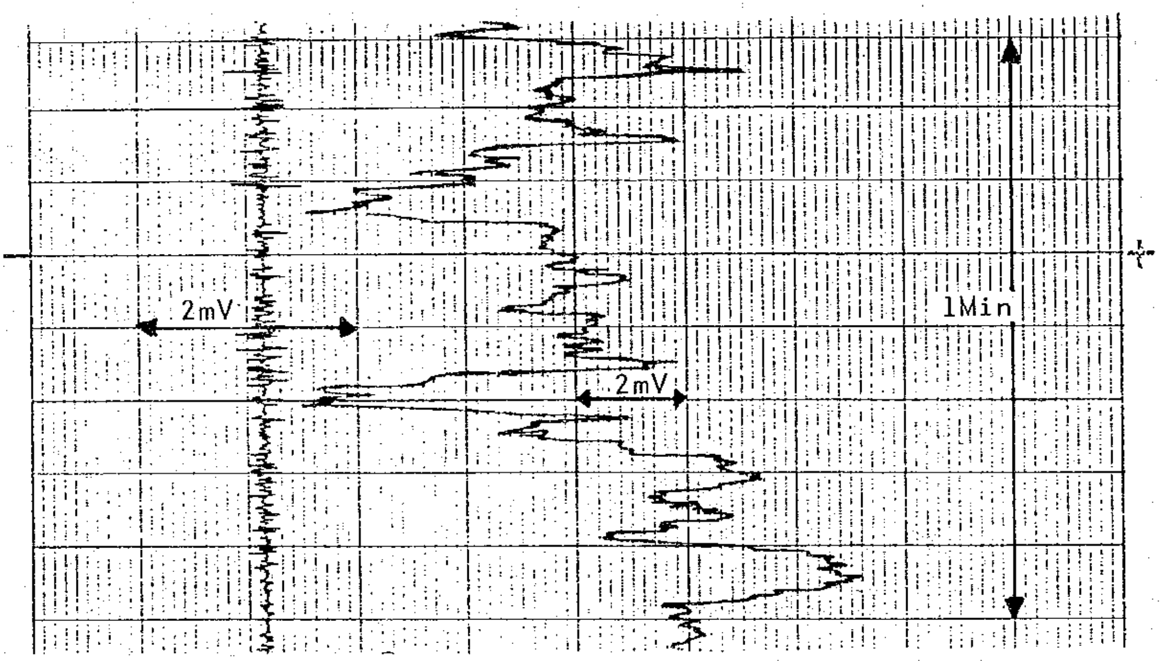

Fig. II–4–3 Noise Wave Form

4–2–2 Survey line

Resistivity survey was conducted along the road. In order to collect as much data as possible in broad area, east – west road from Baguio City to Twin River Junction and to the Agno river and north – south road from Baguio Airport to Philex road and the road along the Agno river were measured.

The road around the Acupan mine is concrete paved as shown in the picture and there are many buried pipes and transmission wires around so that the resistivity survey was not able to be conducted.

Roadside measurement

Paved road near the Acupan Mine

Plan map of the lines are shown on Fig. II–4–4. Survey points are set every 100 m apart in continual number.

Line name and their lengths are as follows.

Name	Line Length	
A	20.0 km	East Baguio – Agno River
B	16.0	North Baguio Airport – Philex Road
C	8.4	Tank – Balatoc – Itogon
D	4.0	Tuding – Baco – Kelly
E	5.9	Twin River Junction – Itogon Mine
F	7.3	Agno River
G	4.0	
H	2.0	
I	2.0	
Total	69.6 km	

Furthermore, in Dalupirip 1000 m line was measured by Schlumberger and Dipole-Dipole configuration, and the total line length is 70.6 km.

4–3 Method of Interpretation

Interpretation of the survey results were made by making pseudosections of each lines and resistivity plan maps. The apparent resistivity values of the dipole-dipole method were plotted on the pseudosections as shown on Fig II–4–2. Contour lines of 50,100,200, and 500 ohm-m were used to determine the shape of the anomalies.

Since the survey was carried out along the roads, the distances of the resistivity lines are very far from each other that the detected anomalous zones could not be correlated with each lines. In general, analyses of the isoresistivity maps from each depth of penetration were made to delineate the alteration zones.

4–3–1 Resistivity of the Rocks

Fifty three (53) rock samples were collected and cut into rectangular blocks and calculated for its cross-sectional area, length and potential difference. Resistivity is then measured by supplying weak current to the rock samples (Table II–4–1).

Resistance R of the rock is proportional to the length ℓ and is inversely proportional to the cross-sectional area S as expressed in the following equation:

$$R = \rho \cdot \frac{\ell}{S}$$

This proportional factor ρ is the resistivity and the above equation can be further expressed as follows:

$$\rho = \frac{S}{\ell} \cdot R = \frac{S}{\ell} \cdot \frac{V}{I}$$

The rock samples collected in the area are generally compact and have high resistivity.

4–4 Results of Resistivity Analysis

Geothermal reservoir rocks are usually capped by altered materials characterized by low resistivity values of less than 10 ohm-m while their resistivity value vary from 50 ohm-m to several hundred ohm-m at depths.

The reconnaissance electrical survey covered most part of the survey area and conducted to detect these low resistivity zones of less than 10 ohm-m. However, no extensive low resistivity zones were encountered although lower sub-surface resistivities due to mineral alterations were observed.

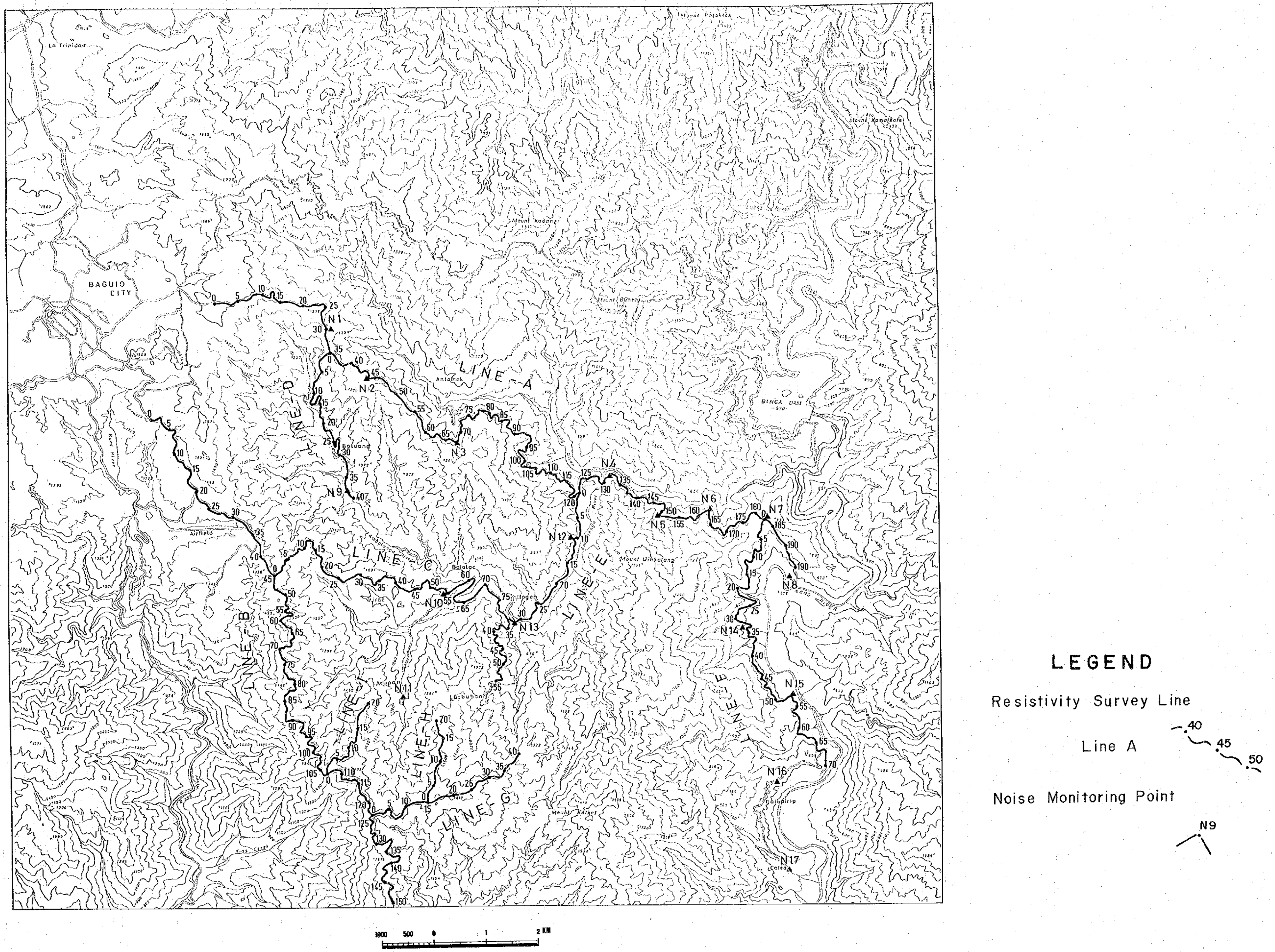

Fig. Ⅱ-4-4 Location Map of Resistivity Survey

Table II–4–1 Resistivity Measurement of Rock Samples

No.	Sample Name	Section (cm^2)	Length (cm)	Current (μA)	Potential (mV)	Resistivity (Ω m)
1	H–1	4,733	2,430	0.1071	93.00	16,906
2	H–1A	4,657	2,580	0.3500	22.05	1,137
3	H–2	4,600	2,490	0.1786	74.00	7,656
4	H–2A	4,634	2,660	0.2750	41.50	2,630
5	H–3	4,675	2,550	0.3036	33.00	1,992
6	H–3A	4,638	2,500	0.2857	42.00	2,727
7	H–4A	4,657	2,580	0.2786	45.00	2,916
8	H–5	4,695	2,540	0.2857	42.00	2,717
9	HUG–5	4,638	2,385	0.1500	78.75	10,209
10	H–6	4,695	2,345	0.2321	54.50	4,700
11	H–7	4,734	2,260	0.3857	15.75	855
12	H–8	4,657	1,980	0.3857	13.45	820
13	H–9	4,676	2,400	0.3570	20.50	1,118
14	H–11	4,657	2,370	0.1786	70.00	7,703
15	H–11a	4,676	2,200	0.1679	75.25	9,528
16	H–12	4,657	2,270	0.2460	52.25	4,350
17	H–15	4,638	2,340	0.3607	18.50	1,016
18	H–18	4,657	2,215	0.2571	44.25	3,311
19	H–19	4,119	2,290	0.1460	80.25	9,857
20	H–21	4,380	2,295	0.2893	33.90	2,236
21	H–24	4,600	2,160	0.4214	1.29	65
22	H–25	4,657	2,430	0.2893	39.00	2,584
23	H–27	4,695	2,455	0.2786	44.00	3,020
24	H–31	4,657	2,300	0.1643	74.75	9,213
25	H–32	4,695	2,405	0.1785	72.50	7,925
26	H–33	4,657	2,445	0.2786	43.00	2,940
27	H–34	4,714	2,360	0.4000	5.95	297
28	H–35	4,695	2,255	0.1821	69.25	7,915
29	H–36	4,695	2,320	0.2036	65.00	6,461
30	H–38	4,676	2,250	0.2460	19.80	1,669
31	H–39	4,714	2,040	0.2250	57.50	6,000
32	H–41	4,676	2,295	0.2821	39.20	2,823
33	H–42	4,714	2,215	0.2214	58.75	5,646
34	H–43	4,695	1,870	0.2321	52.50	5,678
35	H–46	4,676	2,390	0.2429	52.00	4,189
36	H–47	4,695	2,330	0.2430	53.75	4,459
37	H–49	4,712	2,190	0.1786	68.00	8,208
38	H–51	4,695	2,360	0.3285	25.00	1,513
39	H–52	4,714	2,265	0.2500	50.00	4,162
40	H–53	4,714	2,280	0.2000	65.00	6,719
41	HUG–1	4,695	2,290	0.3640	6.40	331
42	HUG–6	4,695	2,130	0.1071	89.75	18,464
43	H–29	4,695	1,970	0.4214	26.20	148
44	1	23,414	6,915	0.1000	95.00	32,167
45	2	13,756	6,765	0.0714	102.00	29,037
46	3	23,586	6,310	0.2143	60.00	10,466
47	4	6,426	6,575	0.2679	44.40	1,620
48	5	13,469	5,300	0.4286	1.08	63
49	7	4,849	3,790	0.2143	61,25	3,657
50	8	45,068	9,295	0.3750	14.25	1,842
51	10	13,854	4,030	0.3929	5.75	503
52	11	23,586	3,215	0.2679	45.00	12,324
53	12	4,700	3,050	0.4286	1.80	65

4–4–1 Analysis of Pseudosections

Line A (Fig. II–4–5)

Resistivity line A is twenty (20) kilometers long and extends from the eastern side of Baguio City at Mansion House, passes south of Antamok Mine and the Twin River junction, to the Agno River. Generally resistivity values decrease to the west of Twin River junction and increase eastwards to the Agno River. The results conform with the geology of the area where the low resistivity zones coincide with the alteration zone and the younger less densed-sedimentary rocks; and the high resistivity zones are attributed to the massive and dense rocks.

Low resistivity zones (< 50 ohm-m) were delineated on stations 0 to 10 around the Mansion House and superficially on stations 24 to 56.

A subsurface low resistive zone was also detected west of the Twin River junction. Resistivity increases east of the junction with the intermediate values of 50 to 200 ohm-m occurring west of the junction and the resistive values of more than 200 ohm-m detected to the east.

Line B (Fig. II–4–6)

The line starts south of Camp John Hay Air Station, passes through the Baguio Airport to the Philex Copper Mine in the south. It is located along the road and stretches for 16 kilometers.

Low resistivity zones (< 50 ohm-m) were observed from station B–4 to station B–30. It conforms with the alterations on the area and extends at depths.

Resistive values of more than 500 ohm-m were encountered from stations B–90 to station B–105 and south of Station B–150. This coincides with the intrusive bodies like the andesite porphyry formations in the vicinity.

Resistivity of 100 to 500 ohm-m characterized the other parts of the area where it reflects the resistivity values for andesites.

Line C (Fig. II–4–7)

The line cuts the survey area from east to west, passing through Virac, Balatoc and Itogon. It is 8.4 kms. long.

Low resistivity zone is distributed in stations C–55 to C–68 and reflects the mineralization in Balatoc.

A low resistivity zone was also found near the Itogon bridge, where the hot spring is located, and this zone is assumed to extend at depths. A high resistive body which is believed to be caused by the presence of andesite porphyry was also noted at station C–70.

Line D (Fig. II–4–7)

This line from Tuding to Baco-Kelly mines is four (4) kilometers long. Low resistive zone is observed at the southern half of this line from station D–30. Resistivities of less than 30 ohm-m are detected which are caused by alterations due to mineralization.

Line E (Fig. II–4–8)

The line starts from the Twin River junction and passes through the Itogon town proper to the Itogon-Suyoc Mine. The total length of the line is 5.9 kilometers.

Low resistivity zones are distributed in stations E–33 to E–41 and north of Itogon bridge at station E–38 to E–44 which is south of the geothermal manifestations at C–82 which also indicates low resistivity. These low resistivity zones are related to the geothermal alteration in the area.

Line F (Fig. II–4–8)

This is 7.3 kilometers long going south to Dalupirip along the Agno river. Although patches of low resistivity values were noted along stations F–30 to F–52, there were no extensive low resistivity zones encountered in this line.

Line G (Fig. II–4–9)

The line is located along the ridge south of Acupan-Itogon mine at Mt. Ampucao, passing through the relay station of PLDT. It is four kms. long.

Resistivity values of less than 200 ohm-m were encountered along stations G–6 to G–24 and less than 100 ohm-m in G–6 to G–8. This is due to dacite mineralization south of Acupan mine and which is also manifested along lines H and I.

Line H (Fig. II–4–9)

This line was planned along the ridge. The survey was carried out after only two (2) kilometers due to the increasing noise from the mine site and steep topography. Since, moderate values were encountered, it is assumed that the place has undergone alterations.

Line I (Fig. II–4–9)

Low subsurface resistivity was encountered at station I–5 but this may be due to the drainage in the nearby village. Moderate values of less than 200 ohm-m were also measured southwest of Acupan mine.

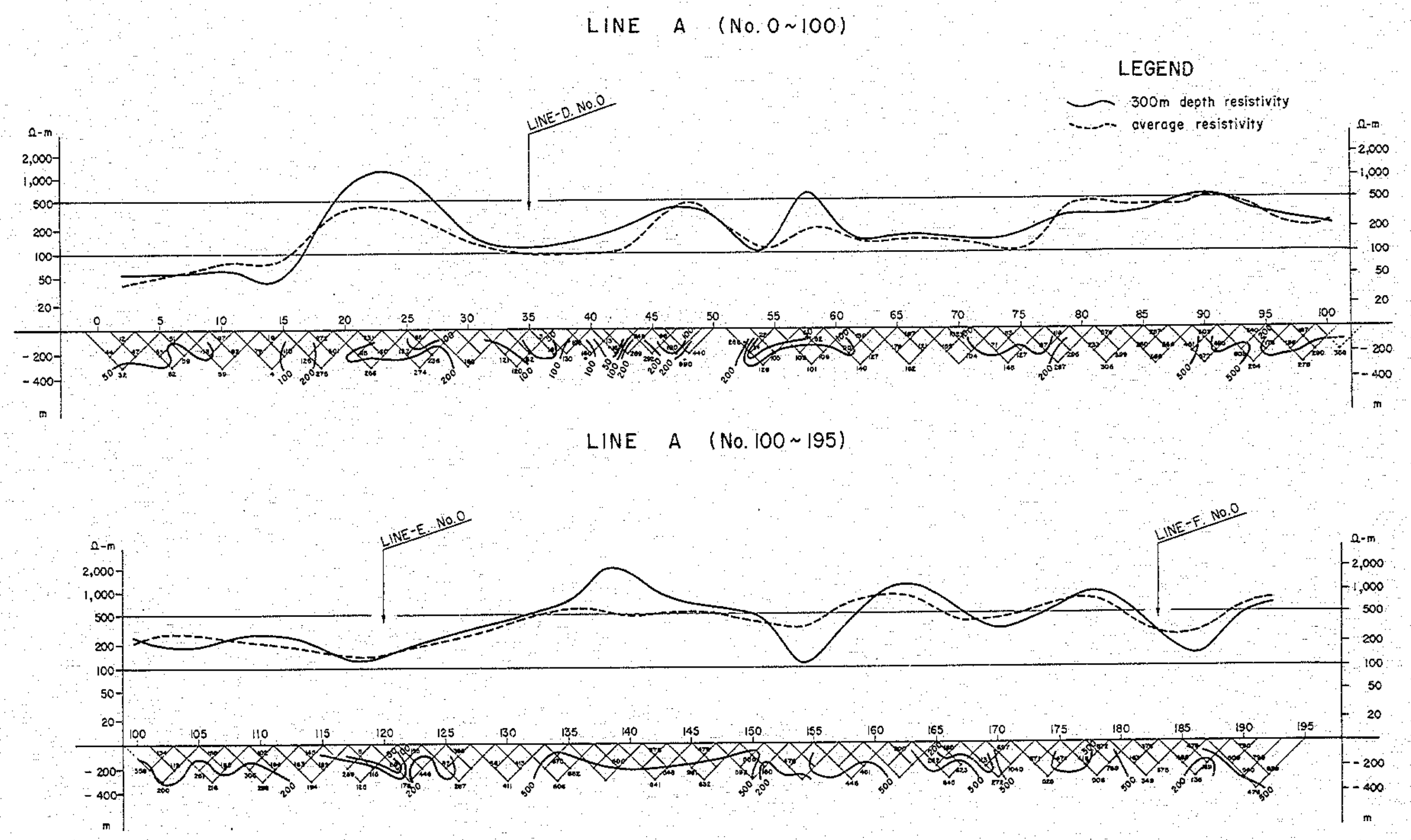

Fig. II–4–5 Apparent Resistivity Section Line A

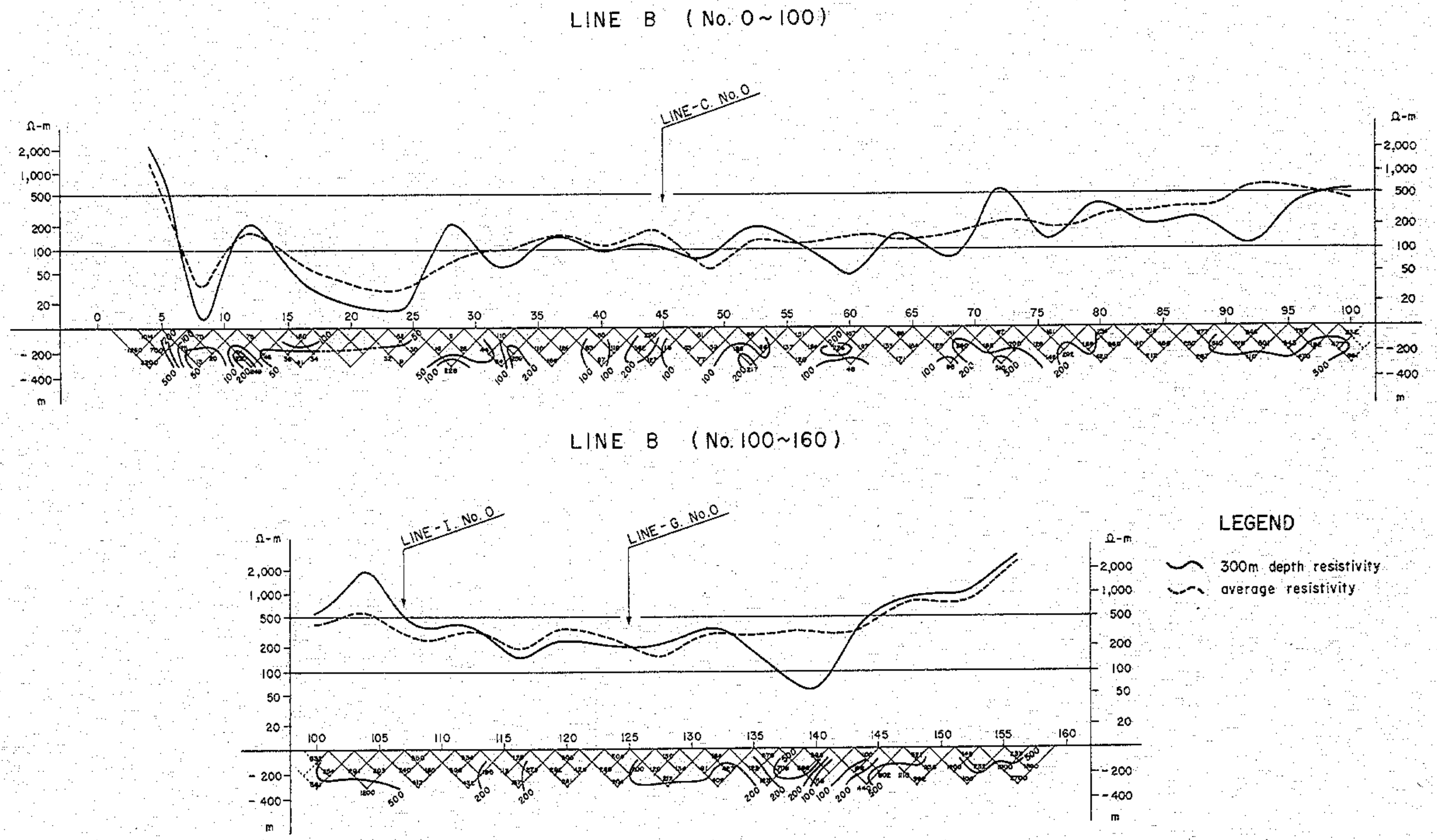

Fig. II–4–6 Apparent Resistivity Section Line B

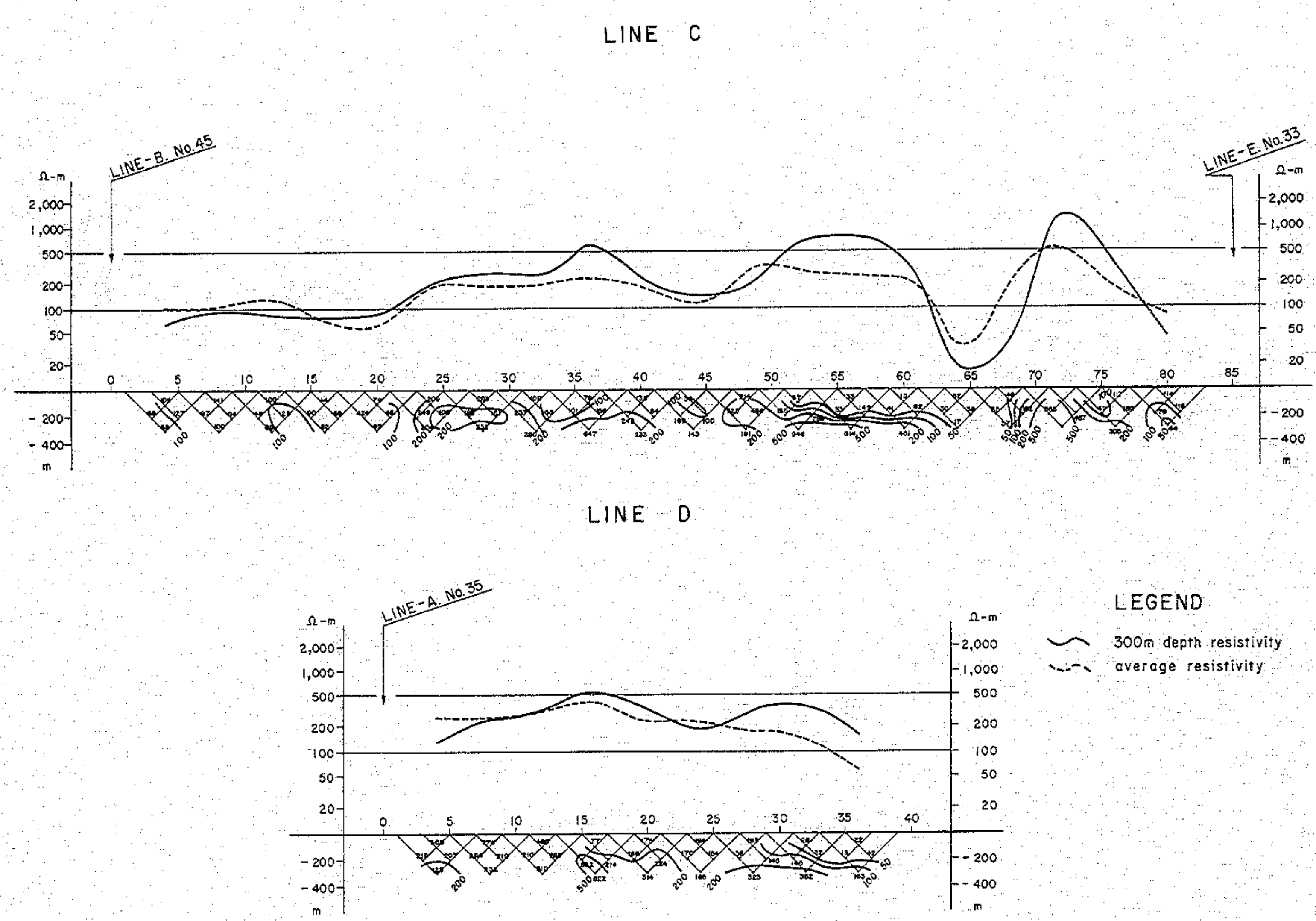

Fig. II–4–7 Apparent Resistivity Section Line C & D

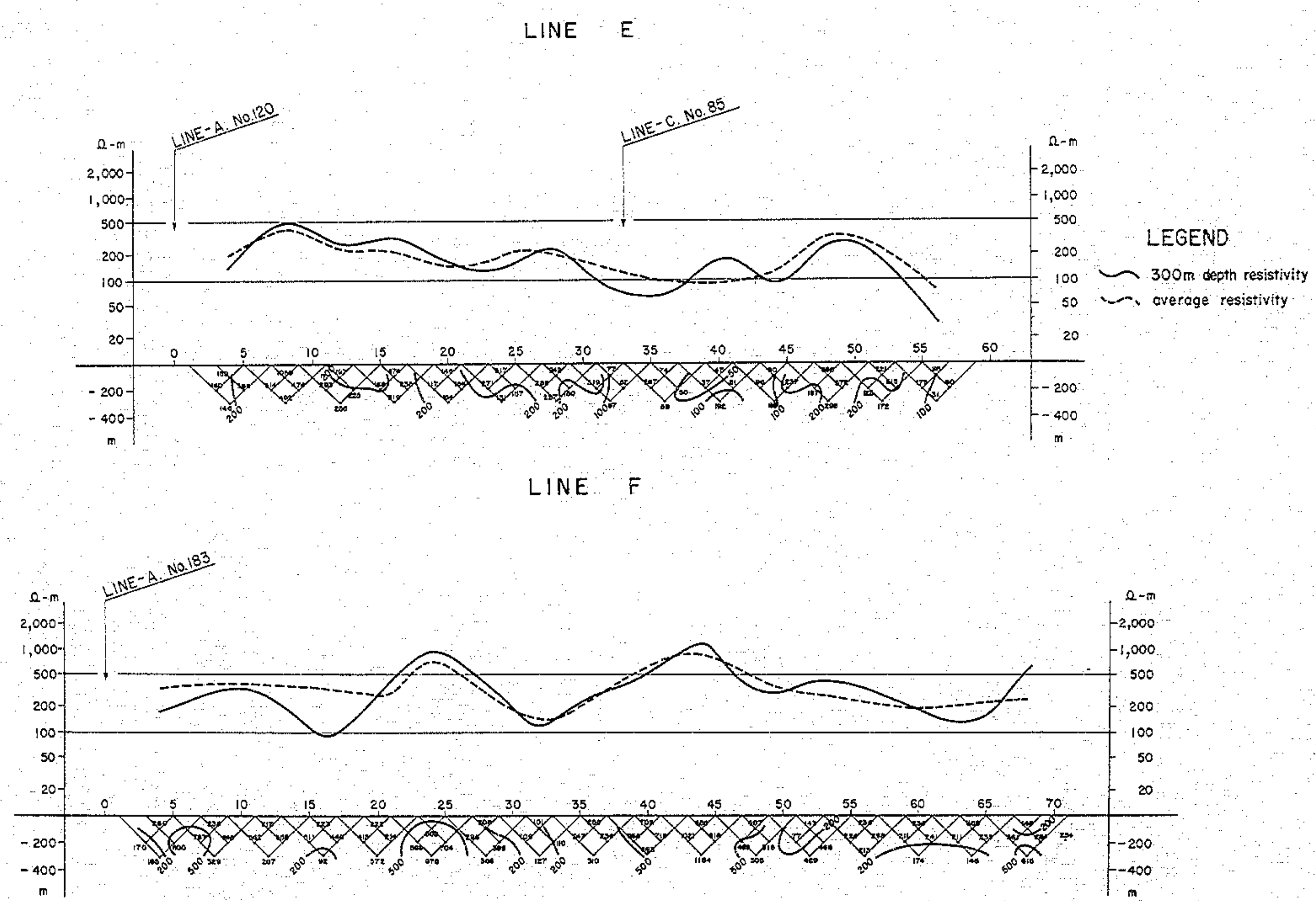

Fig. II—4—8 Apparent Resistivity Section Line E & F

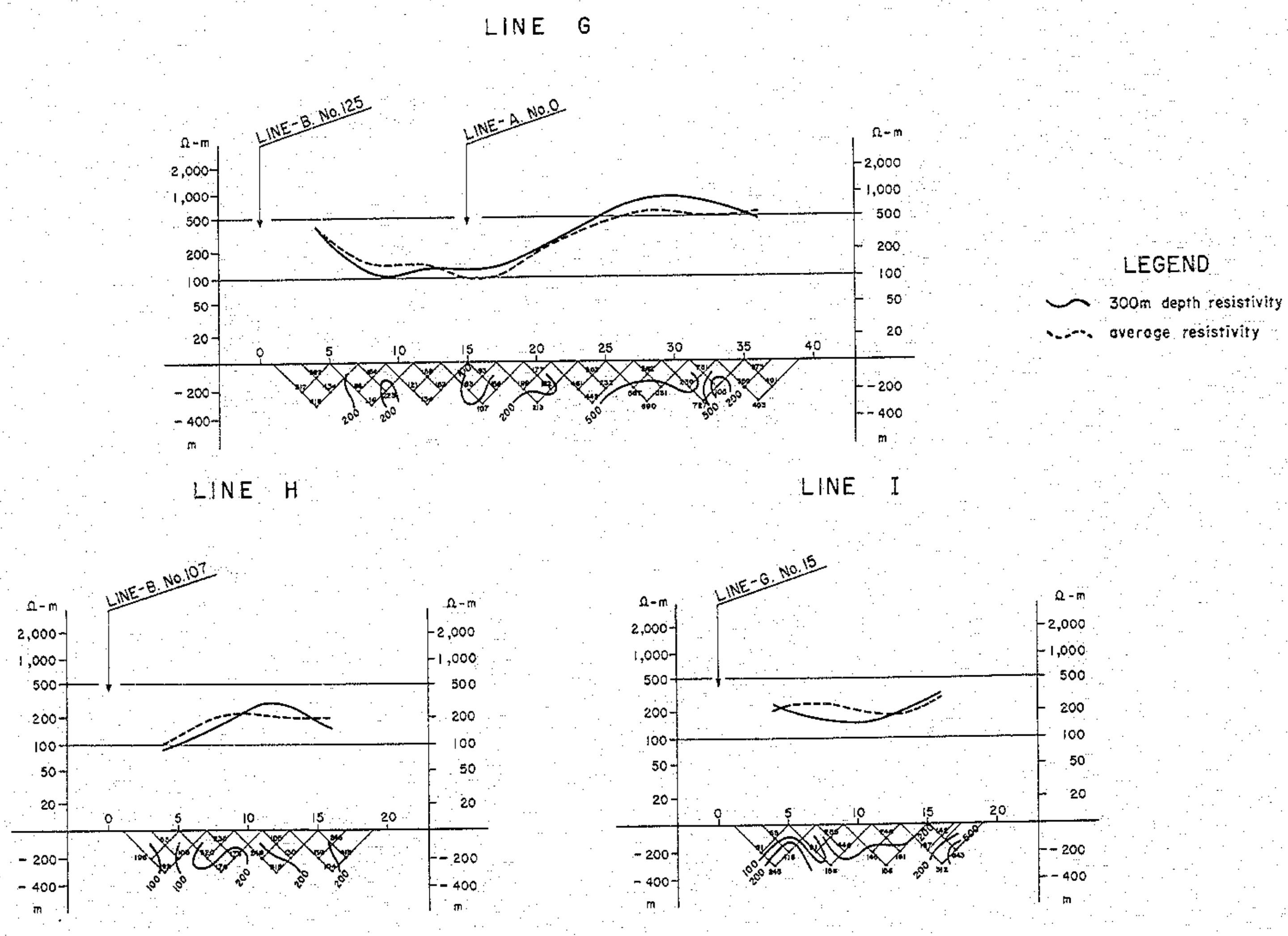

Fig. II–4–9 Apparent Resistivity Section Line G, H & I

4–4–2 **Plan Analysis**

In this survey, three resistivity depths (100m, 200m, and 300m) were measured by changing the electrode spacing. The measured values are plotted in the form of pseudosection maps in order to understand the distribution of the resistivity for each depth, as shown in Fig. II–4–10. It was impossible to draw successive contour since distances among each survey lines were wide apart. However, resistivity anomalies were found in the following locations:

1. Mansion House: Characterized by low resistivity zone with value of less than 50 ohm-m from the surface to the depth of Line A, station No. 15. It is believed that tuff and the Klondyke formation and thick mudstone have influenced by argillization which could have caused this anomaly.

2. Baguio Airport: Represented by shallow to deep low resistivity zone. The topography is similar to that of No. (1), but Argillization to montmorillonite is intense and more of an alteration due to gold mineralization than to hydrothermal.

3. Balatoc Mines: Typified by low resistivity zone of less than 50 ohm-m. It is encountered in Line C from station 50 to 70. The slug from mine tunnels which is located in the center of ore deposit might have caused some of the low resistivity values obtained.

This anomaly tends to spread towards the east at depth and possibly the extension of the low resistivity zone within the Itogon Bridge. Deep low resistivity values around the geothermal manifestations in Itogon Ranges from 40 to 80 ohm-m.

4. Baco-Kelly Mine: Represented by low resistivity on the northern part of Line D to station 50 to 60 of Line A. This is considered to be the extension of low resistivity zone encountered in Line A from station 50 to 60 near Antomak Mine and possible reflection of the mineralization in the area.

5. Acupan Mines: Localized by low resistivity anomaly in the south. The expected low anomaly within the Mines was not detected due to the location of Line H and I, which were planned for the area. Both lines are situated along the ridge and lateral effect of the topography accounts for the high values encountered.

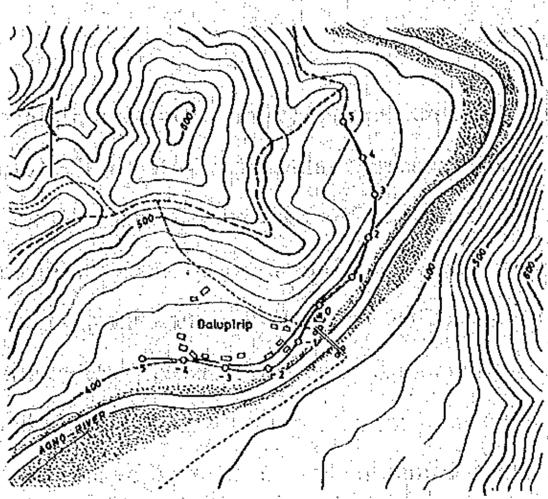

Fig. II–4–11 Location Map of Dalupirip Line

4–4–3 Electrical Survey in Dalupirip

In order to confirm the range and distribution of geothermal alteration zone, resistivity change towards depth was measured by Schlumberger and dipole-dipole method where hot spring manifestation, south of Line F, in the Agno River bank, is located. The survey line starts 100 m north of the Dalupirip bridge as 0 point, 500 m to the north and south of a total length of 1,000 m. Survey points are -5, -4, ...to 0, ...4, 5, with interval of 100 m.

Dipole-dipole Method

Apparent resistivity was measured only up to the depth of 250 m due to electrical noise in the area. The apparent resistivity values (using 3Hz current) vary from 7 to 260 ohm-m and a remarkable low resistivity is found at the center of the survey line. The center of strong low resistivity of hot spring alteration is located between the surveying points, 0 and 1 and an apparent depth of 100 m. Center of subsurface low resistivity is found in the north, around the survey point, 2.

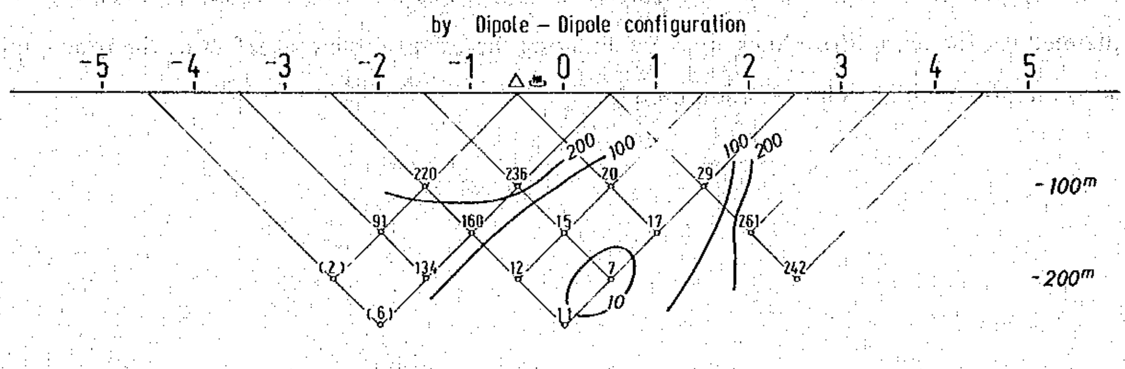

Fig. II–4–12 Apparent Resistivity Section at Dalupirip

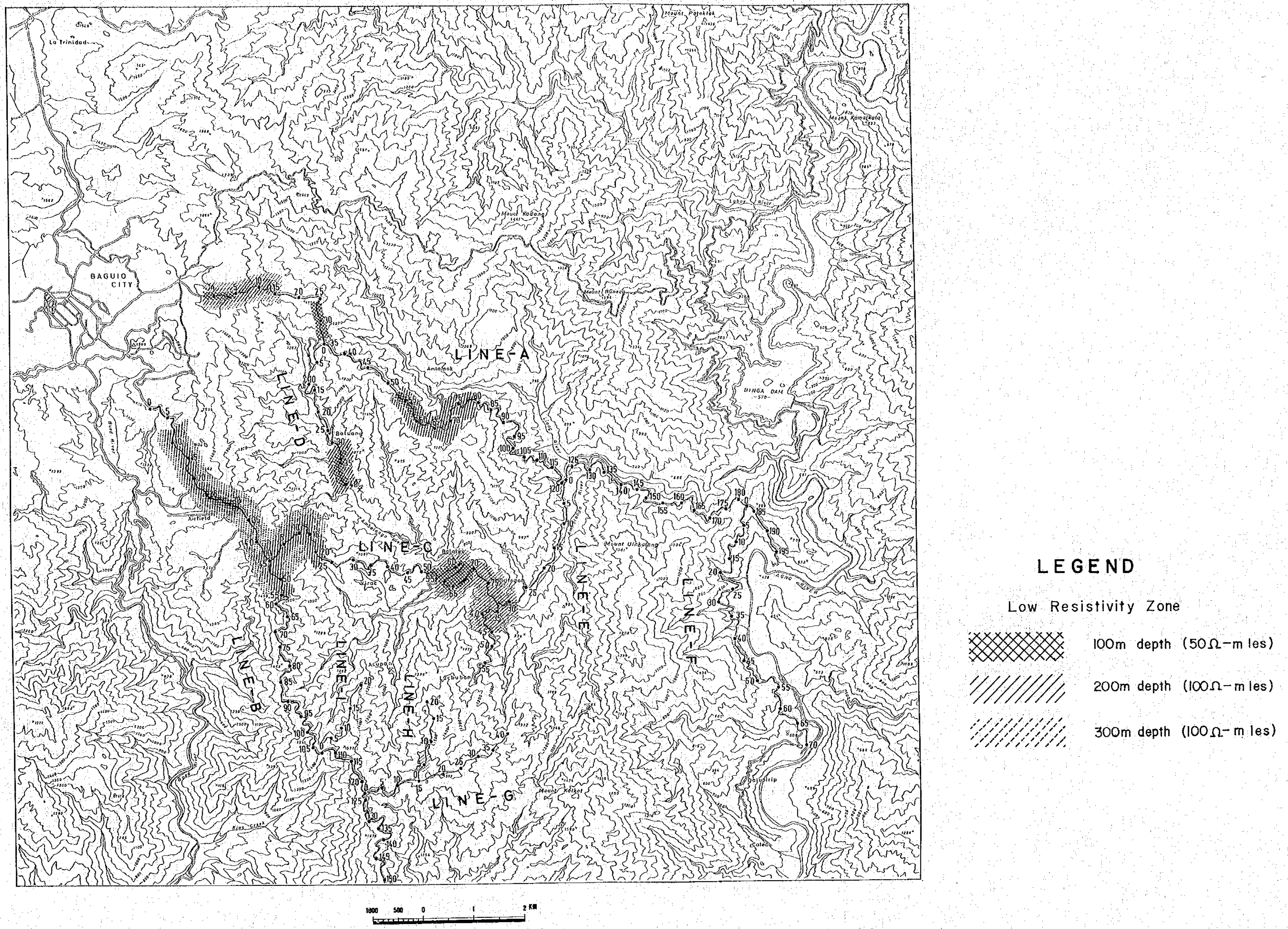

Fig. II-4-10 Plan Map of Resistivity

As shown in the above figure, a strong possibility of weak zone is detected leading the hot spring into NNW-SSE trending direction.

Schlumberger Method

Electrical sounding using the Schlumberger array configuration was also carried out to determine the vertical change of resistivity. A transmitter current of 0.1 Hz was used with the potential difference measured through a pen recorder. The apparent resistivity varies from 50 to 150 ohm-m. Resistivity increases below the 50 meters-depth which confirms that the thermal manifestations arc superficial.

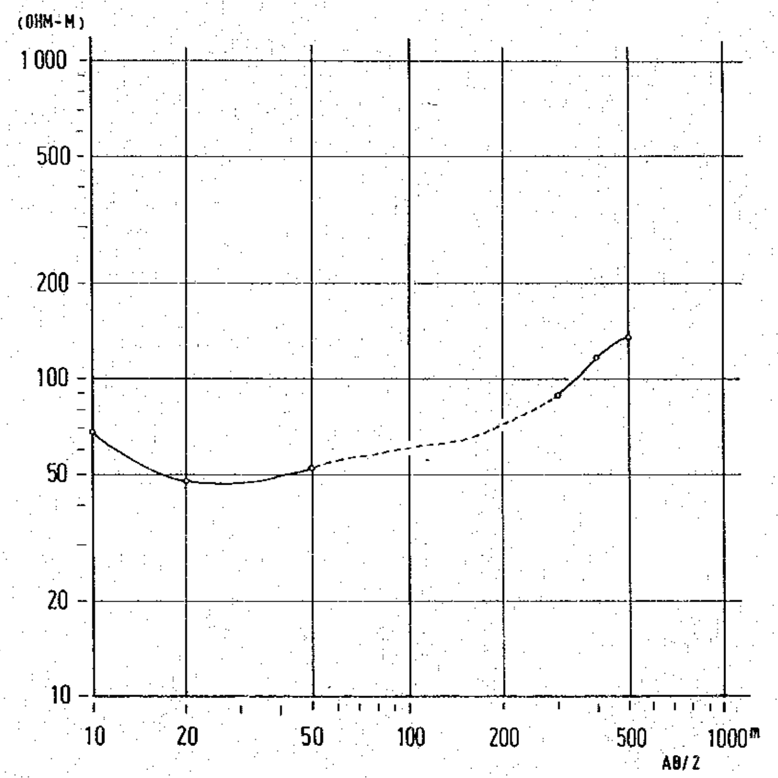

Fig. II–4–13 Vertical Electrical Sounding Curve at Dalupirip

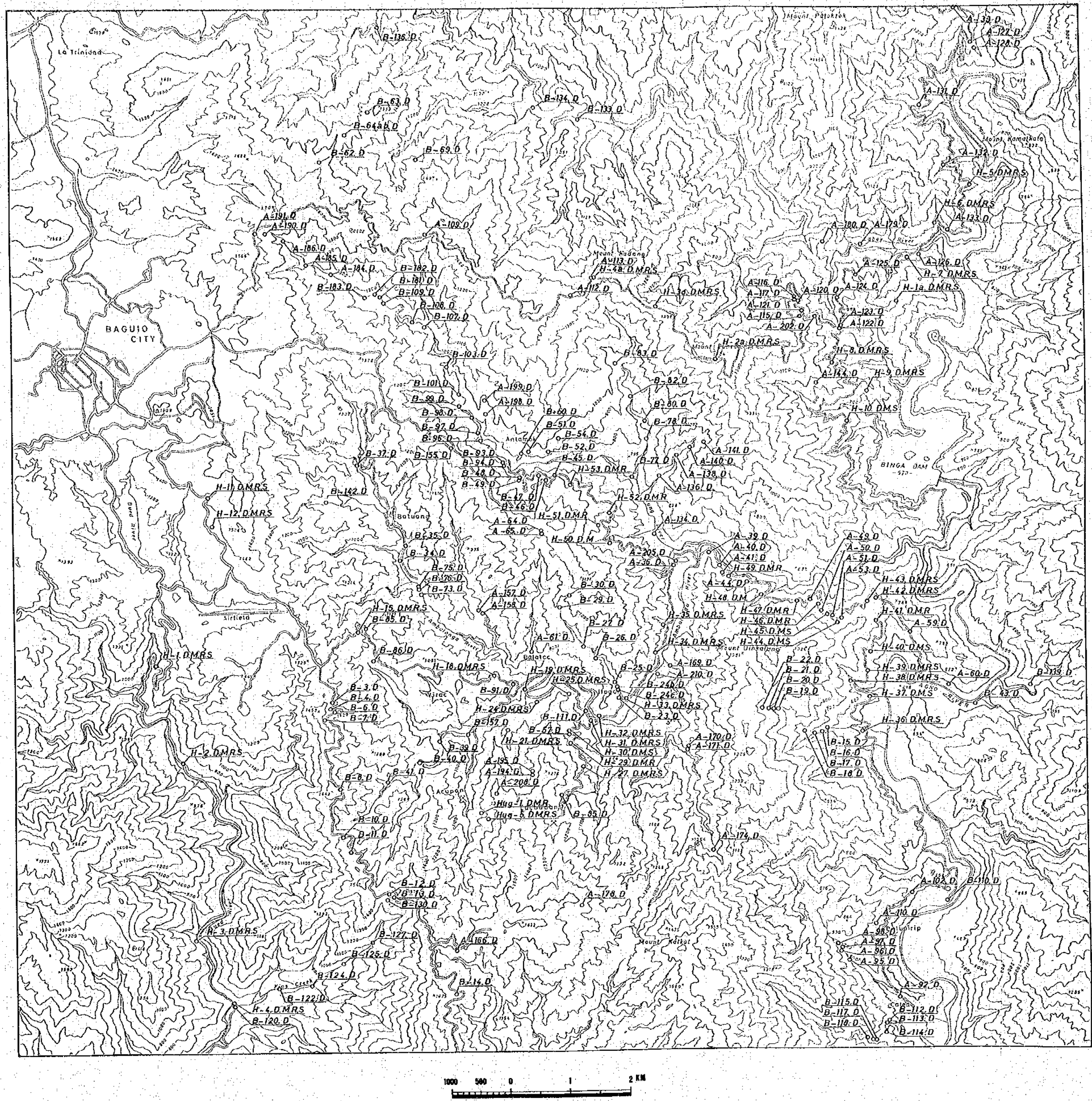

D : Density
M : Remnant Magnetism
R : Resistivity
S : Magnetic Susceptibility

Fig. II-4-14 Location Map of Collected Rock Samples

PART Ⅲ SUMMARY

CHAPTER 1 SUMMARY

CHAPTER 1 SUMMARY

1–1 Summary of Geological Survey

1) Stratigraphy: It is as follows from lower to upper;
Dalupirip metamorphic rocks (Da), Pugo formation (Pu), Columbus formation (Co), Zigzag formation (Zi), Klondyke formation (Kl), Rosario formation (Ro) and Balatoc formation (Bp). The Balatoc plug is composed of dacitic volcanic pyroclastic rocks and is assumed to be a vent breccia. Age determination shows about 0.8 to 1.0 Ma. of early Pleistocene. No dacite dome of late Pleistocene as seen in Buguias and Daklan is exposed in the Acupan–Itogon area.

2) Geological structure: The uplifted zone at the western part of the Buguias and Daklan area extends southwards to the central part of the Acupan–Itogon area. Many geothermal manifestations of the Acupan–Itogon area are mainly located on the western limbs of the uplifted zone, which are bounded by the eastern periphery of the western subsided zone. Structually the project area is emphasized by a central N–S trending uplifted zone, where two subsided zones are located on both sides. These are dislocated trivially by NE–SW and NW–SE trending fractures.

Both geothermal manifestations at the Acupan mine and the Itogon bridge are associated with dacite plugs and ore veins which strike NE–SW. And the Klondyke hot spring is located at the southwest extension of this trend. The NE–SW trending structure is harmonic with the Virac granodiorite intrusions and also with the southern end of the basin structure of Klondyke formation.

Concerning about the Laboy hot springs and Dalupirip hot springs, they are controlled structurally by NW–SE to NNW–SSE trending faults.

3) Volcanism: The dacitic volcanic rocks at the Acupan and Itogon area are assumed to be the heat source of geothermal fluid. According to the result of fission track radiometric age measurements of dacite rock samples, it shows about 0.8 to 1.0 Ma. and it belongs to early Pleistocene of Quarternary age.

4) Geothermal manifestations: The most impressive among the many geothermal manifestations in the area include: the Laboy hot springs which had been found newly during this survey, the hot springs at the Acupan mine and at the Itogon bridge.
The hydrothermal alteration of wall rocks within the investigated area are categorized into four as follow: genetically associated with the porphyry copper mineralization; genetically associated with the mineralization of gold; genetically associated with geothermal fluid; and genetically associated with diagenesis. The hydrothermal alteration of wall rocks here is a duplicate of

these genetical conditions. The zonation of alteration is as follows from inner to outer periphery of intermediate hypabyssal complexes which brought gold mineralization at the Baguio gold mine and at the Baco–Kelly mine: sericite zone, cristobalite alunite zone and montmorillonite zone. Wairakite is seen rarely in sericite zone. Alteration associated with gold mineralization is affected by geothermal fluid in the Acupan mine.

5) Current volume and chemical analysis of stream water: It was not possible to get good data to do further studies because the investigation had been done during rainy and typhoon season.

General idea for a reservoir structure of geothermal aquifer is led as follows from geological understandings: (Fig. III–1–1)

1) Heat source: Balatoc plugs of dacitic volcanic rocks whose ages are about 0.8 to 1.0 Ma. of early Pleistocene are assumed to be a heat source of geothermal aquifer at the Acupan mine and the Itogon bridge.

2) Reservoir of aquifer: The extent of geothermal aquifer is controlled by fractures which develop especially at the periphery of the plugs, and also controlled by fractures which strike NE–SW in and around the plugs but outside of the Itogon quartz diorite.

3) Impressive target: The area of the Acupan mine to Itogon bridge is most impressive for further survey.

1–2 Summary of geochemical survey

The survey consisted of geochemical exploration at 1 m–depth to measure temperature, radon and CO_2 gas concentrations, and mercury content in soil. Likewise, geochemical exploration of hot spring waters were undertaken for chemical analysis, isotopic analysis of O and H, and analysis of associated fumarolic gas. The results of this survey are summarized hereafter.

1–2–1 Geochemical exploration at 1 m–depth

As the correlation of the four measured parameters are very weak, the factorial analysis reveals high peculiarities, and it is not appropriate to comment on any factor. Two variables, soil temperature and mercury content, tentatively assumed to reflect the activity of ground geothermal fluids, while the two others rather reflect geological differences. The soil temperature distribution map shows temperatures around the Balatoc Plug of Acupan Mine exceed the mean soil temperature of the whole area by 25.8°C, 1.2°C more than the standard deviation. The mean value of mercury content in soil is 83 ppb (1.92 in logarithms) and the standard deviation, calculated after conversion to logarithms is 0.65. The mercury content in soil exceeds this mean

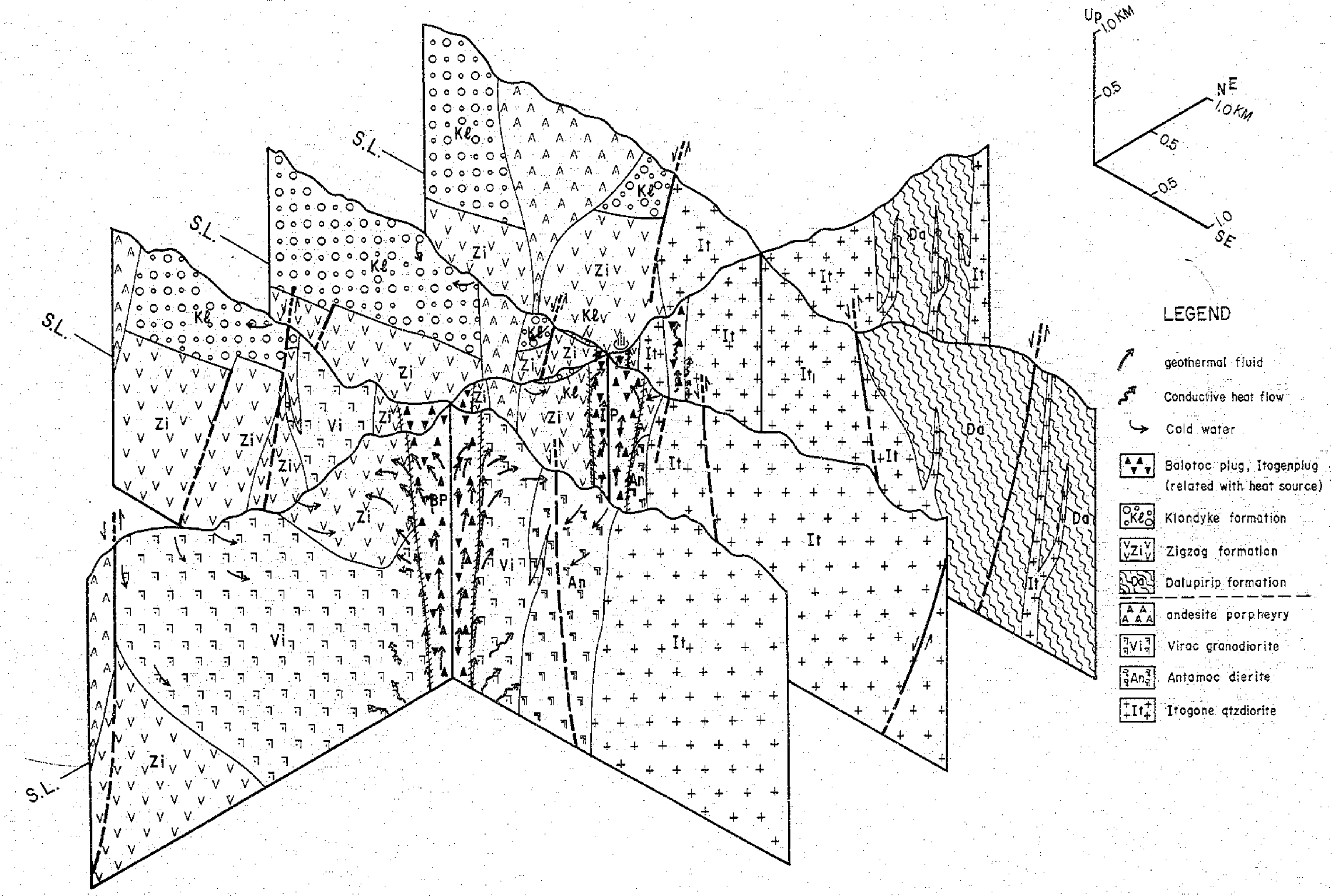

Fig. Ⅲ-1-1 Structural Conception Model of Acupan-Itogon Geothermal Area.

value by more than the standard deviation, that is to say it is higher than 372 ppb (2.57 in logarithms) around Acupan, Itogon and Virac. This zone with high mercury contents corresponds well with the geothermal area shown by the temperature distribution map. With regards to mineralization and mercury enrichment, it seems that it does not relate with copper mineralization. It is possible that the gold mineralization caused a mercury enrichment, and the mercury content map would consequently represent the distribution of hydrothermal activity. On the other hand, radon concentration distribution shows a large positive anomaly with concentration up to 264 $n/mm^2 \cdot 30$ days, associated with andesites and granodiorite-porphyries around Batuang. Whereas, radon concentrations around 15–50 $n/mm^2 \cdot 30$ days, from Acupan Mine to Itogon hot spring show no clear evolution. It is most probable that, by reducing the area of investigation and increasing the number of measurement points of radon concentration, we can obtain valuable informations about the repartition of geothermal fluids underground. Because the soil of the investigated area are very thinly developed, the measurement of CO_2 concentration in soil air is not an appropriate exploration tool in this area.

1–2–2 Geochemical exploration of hot spring water

Four types of water have been recognized on the basis of their chemical compositions among the hot spring waters of this area.

a) The dominant ions are Cl^- and $Na^+ + K^+$; the geochemical temperatures are high: T_{SiO_2} from 147 to 229°C, $T_{Na\text{-}K\text{-}Ca}$ from 193 to 236°C. Since shifts are observed in isotopic composition of O, these waters are thought to be of deep origin or to be close to hot water of deep origin. Waters of this type are found in the Balatoc Plug (Acupan Mine), and locally in Itogon hot spring and Antamok Mine.

b) SO_4^{2-} and Ca^{2+} as dominant ionic species; very low geochemical temperatures; H and O isotopic ratios plotting on or near the meteoric water line. These waters are thought to have formed by dissociation of SO_4^{2-} from the deep hot water followed by mixing with surface or shallow ground waters and subsequent dissolution of Ca^{2-} from rocks. Waters of this type are found in Acupan Mine outside Balatoc Plug, in Antamok Mine and in Laboy hot springs.

c) SO_4^{2-} and $Na^+ + K^+$ as dominant anions and cations; relatively high geochemical temperatures: T_{SiO_2} from 91 to 209°C, $T_{Na\text{-}K\text{-}Ca}$ from 54 to 216°C; yet the δD and $\delta^{18}O$ values plot near the meteoric water line. Waters of this type may be thought of as representing a transitional state between type a) waters, which are close to deep hot waters, and type b) waters, which show a strong influence of surface waters. Type c) waters are found in Dalupirip and in most of the Itogon hot springs.

d) Cl^- as dominant anion, $Na^+ + K^+$, and especially Na^+ as dominant cations; low geochemical temperatures; T_{SiO_2} from 46 to 144°C, $T_{Na\text{-}K\text{-}Ca}$ from 27 to 68°C; O and H isotopic ratios plotting on the meteoric water line. The associated gases show extremely low concentrations of CO_2 and H_2S, and these are probably not related to the Quarternaly volcanic activities. They are found in Asin, Klondyke, and Pugo.

If we take accurate classification of hot springs and the formation processes assumed for each type of hot water, the future geothermal exploration should concentrate on the relatively large area, from Acupan to Itogon, where hot springs of type a) are located.

1–3 Summary of Gravity Survey

As the roads are so developed in the area of 180 km^2 for gravity survey, 310 gravity stations have been planned and scattered despite its steep topography among which are 298 levelling points and 12 microbarometric levelling points.

High accuracy corrections such as tidal, instrumental, drift, latitude, free-air, topography, and Bouguer have been made.

Consequently, Bouguer anomaly map corrected by an assumed density of 2.60 is found to be the best to explain the geological structure of the area, and from this, several filtered maps of band-pass-filter are made for the interpretation of the geological structure.

Results of the interpretation are as follows:

(1) Average density of the rocks in the survey area is around 2.70 and the difference in each is negligible. Accordingly, the difference in gravity anomaly is small and its maximum and minimum values are 77 and 49 mgal respectively.

(2) Low gravity zone from the center of the area to SSE coincides with the distribution area of Itogon quartz diorite.

(3) According to the residual map of $\lambda = 0.25 \sim 2.1$ which describes the structure shallower than 1,500 m, small scale gravity highs surrounding the above-mentioned low gravity zone are seen. The southwestern one corresponds to Zigzag formation, southeastern one to Dalupirip metamorphic rocks, and the eastern one to Pugo formation. The other gravity highs are due to intrusive rocks with comparatively high density.

(4) Residual gravity map of $\lambda = 2.1 \sim 10.2$ describes the structure of 1,500 ∿ 3,000 m. High gravity anomalies seen along the southwestern and eastern edges of the area suggest Zigzag and Pugo formations in the depths. A large scale gravity low found in the center of the map is not due to the basin structure with several faults around, but Itogon quartz diorite which has a smaller density than the surrounding rocks and seems to extend to the depths.

(5) No eminent fault structure or subsided zone which may relate to geothermal reservoir has been detected.

(6) A small scale gravity low is seen in the east of Acupan mine, where geothermal manifestations are found. Around the Balatoc plug are Virac granodiorite, Antamok diorite and gabbro intrusives which all have comparatively high density. This suggests that the rocks around the plugs have well-developed fractures and the total density of the rock body is higher than that of the collected samples.

1–4 Summary of Electrical Survey

In this survey area are many active mines such as Acupan and Itogon where the resistivity survey is often disturbed by much electrical noise caused by tramcars. Thus, resistivity sounding cannot be conducted. Electrical reconnaissance was adopted to find the resistivity change in comparatively shallow zone of 200–300 m.

Topography of the area is so steep that nine survey lines are planned and executed all along the road with the total survey line length of 69.6 km.

Current supplied to the ground is a square wave of 1 to 2.5 ampere current of exactly 3 Hz in order to remove the noises by means of sharp band-pass filter.

By plotting the results on both sections and the plan maps and comparing these with geology of the area, the following conclusions are derived:

(1) Apparent resistivities of the area range from 50 to 1,000 ohm-m with high resistivity of more than 500 ohm-m were detected mainly due to the alteration of gold mineralization.

Low resistivity due to geothermal alteration was found near the Itogon bridge, which does not seem to develop in wide range.

(2) East of Baguio City (A–0 ~ A–15) and near Baguio airport (B–4 ~ B–30) wide low resistivity zone are confirmed where tuff and mud stone of Klondyke formation are strongly argillized.

(3) Low resistivity zone related with slug and trailing of the mines were detected around Balatoc (C–50 ∿ C–70), Antamok (A–50 ~ A–60), and Baco–Kelly (D–30 ~ D–40).

(4) Around Balatoc plug where very low resistivity due to geothermal alteration had been expected, resistivity could not be conducted because of paved road to the mine site and the buried iron pipes and wires.

(5) Vertical electric sounding was conducted at Dalupirip hot spring and found that the hot springs seem to come up along the fractures running in N–S to NNW–SSE direction. But judging from an increasing resistivity towards the depth, geothermal alteration is not very dominant.

CHAPTER 2 CONSIDERATION OF GEOTHERMAL SYSTEM

CHAPTER 2 CONSIDERATION OF GEOTHERMAL SYSTEM

2–1 Geological Structure and Geothermal Fluid

The objective of geothermal exploration is to estimate the outline of size, shape and productive amount of the geothermal reservoir, therefore, geological, geochemical and many kinds of geophysical techniques are conducted to locate the heat sources of geothermal system which could be the potential reservoir.

In world-wide, the fact that the geothermal sources mainly exist in grabens are due to good geological conditions for storage of water which is the carrier of heat.

In general, the aquifer basin structure is controlled by the structure of non-permeable and permeable layers, but since high temperature water has very low viscosity, it is believed that perfect non-permeable beds do not exist unless these beds have no fructures. Hence, the structures that control geothermal reservoir are not the characteristics of individual geological formation, but rather the combination of large scale geological structures.

The effects of flushing of geothermal fluid from the well are generally considered to affect within several kilometers. The subsurface water movement is not controlled by the porosity in a narrow sense, but is controlled by the porosity in a broad sense which includes the fine fractures. These fine fractures can not be neglected when high temperature fluid flow with low viscosity coefficients is considered. And it is not necessarily meant that more surface manifestations suggest more favorable high temperature fluid at depth.

Classification of geothermal system has been studied by many researchers but no satisfactory classification is done. Some of them are classified based upon the geological environment, and the others depend upon the geophysical characteristics which control the water circulation.

In general, high-temperature geothermal system can be found in Quaternary volcanic zone, and each geothermal electric power generation areas in Japan, New Zealand, and Philippines are not the exceptions. But high temperature geothermal zone in Larderello of Italy and in Imperial Valley of the United States can not be found in young volcanic zone considering the heat source in geothermal system, but can be found in metamorphic rock, dolomite marble, shale or in delta sedimentary rock.

Size of the geothermal system is multifarious. In some volcanic zone, it is less than 2 to 3 km^2. In lava extrusion zone, the activity occurs in small range even though its surface geothermal manifestation is very predominant.

In volcanic zone of grabens, the geothermal system is developed within several hundred km^2. For the area which has narrow geothermal system, it is believed that most of them are relating to the uplift zone in geological structure and hot rock body is generally shallow and its geothermal system tends to be controlled by fault structures and extends in certain direction in general.

The interpretations of exploration results for this area are carried out with reference to the above-mentioned facts.

2–2 Geothermal potentiality

1) The geothermal system for this area shift to locate to the west from S–N trending of Quaternary volcanic zone in North Luzon passing through adjacent area of geothermal manifestation of Buguias and Daklan. Hence, there is no large scale dacite dome (10–20 thousand year old) in this area and it is considered to be the geothermal system relating to the activity of vent breccia. The development of plug is analyzed about a million year-old, and is related to rather old activity.

2) These plugs are deeply related to the development of the geothermal system and also show close relationship with the gold mineralizations. And this gold mineralization is believed to be continuous even now.

These plugs having NE–SW trend are developed in transformation point between the eastern area where basement are exposed and the western area which has thick Tertiary formation. And this trend of plugs in this area matches with the direction of vein fractures.

3) Geothermal activity in this area which can be the subject for further survey is correlated with the geothermal manifestation zone relating to the development of plug. This geothermal manifestation zone has no relationship between large scale basin or collapse structure. It is related to fault structure and fracture system in the area from intrusion of plugs.

4) The hot spring water in this area is categorized as NaCl and $CaSO_4$ types. The one in the plug belongs to NaCl type with T_{SiO_2} and $T_{Na\text{-}K\text{-}Ca}$ indicating more than 200°C. δD and $\delta^{18}O$ by isotopic analysis show shift and are considered to be deep geothermal fluids.

5) Some of the low resistivities detected by electric survey are mainly due to the alteration of mineralization, but some of them around Itogon geothermal manifestation is considered to be as geothermal alteration. The extent of the depth is not clarified.

6) Regarding gravity survey no typical gravity anomaly for geothermal reservoir structure is shown; however, gravity low matches the distribution of Itogon quartz diorite and local gravity low on the Balatoc plug was confirmed.